

# Cerebral Metabolic Profiling of Hypothermic Circulatory Arrest with and Without Antegrade Selective Cerebral Perfusion: Evidence from Nontargeted Tissue Metabolomics in a Rabbit Model

Li-Hua Zou<sup>1</sup>, Jin-Ping Liu<sup>1</sup>, Hao Zhang<sup>2</sup>, Shu-Bin Wu<sup>1</sup>, Bing-Yang Ji<sup>1</sup>

<sup>1</sup>Department of Cardiopulmonary Bypass, Fuwai Hospital and National Center for Cardiovascular Diseases, Chinese Academy of Medical Sciences, Peking Union Medical College, Beijing 100037, China

<sup>2</sup>Department of Surgery and Center for Pediatric Cardiac Surgery, Fuwai Hospital and National Center for Cardiovascular Diseases, Chinese Academy of Medical Sciences, Peking Union Medical College, Beijing 100037, China

## Abstract

**Background:** Antegrade selective cerebral perfusion (ASCP) is regarded to perform cerebral protection during the thoracic aorta surgery as an adjunctive technique to deep hypothermic circulatory arrest (DHCA). However, brain metabolism profile after ASCP has not been systematically investigated by metabolomics technology.

**Methods:** To clarify the metabolomics profiling of ASCP, 12 New Zealand white rabbits were randomly assigned into 60 min DHCA with (DHCA+ASCP [DA] group,  $n = 6$ ) and without (DHCA [D] group,  $n = 6$ ) ASCP according to the random number table. ASCP was conducted by cannulation on the right subclavian artery and cross-clamping of the innominate artery. Rabbits were sacrificed 60 min after weaning off cardiopulmonary bypass. The metabolic features of the cerebral cortex were analyzed by a nontargeted metabolic profiling strategy based on gas chromatography-mass spectrometry. Variable importance projection values exceeding 1.0 were selected as potentially changed metabolites, and then Student's *t*-test was applied to test for statistical significance between the two groups.

**Results:** Metabolic profiling of brain was distinctive significantly between the two groups ( $Q^2Y = 0.88$  for partial least squares-DA model). In comparing to group D, 62 definable metabolites were varied significantly after ASCP, which were mainly related to amino acid metabolism, carbohydrate metabolism, and lipid metabolism. Kyoto Encyclopedia of Genes and Genomes analysis revealed that metabolic pathways after DHCA with ASCP were mainly involved in the activated glycolytic pathway, subdued anaerobic metabolism, and oxidative stress. In addition, L-kynurenine ( $P = 0.0019$ ), 5-methoxyindole-3-acetic acid ( $P = 0.0499$ ), and 5-hydroxyindole-3-acetic acid ( $P = 0.0495$ ) in tryptophan metabolism pathways were decreased, and citrulline ( $P = 0.0158$ ) in urea cycle was increased in group DA comparing to group D.

**Conclusions:** The present study applied metabolomics analysis to identify the cerebral metabolic profiling in rabbits with ASCP, and the results may shed new lights that cerebral metabolism is better preserved by ASCP compared with DHCA alone.

**Key words:** Antegrade Selective Cerebral Perfusion; Cardiopulmonary Bypass; Metabolic Profiling; Metabolomics

## INTRODUCTION

Cerebral protection during aortic arch repair is of great concern for clinic outcome. Antegrade selective cerebral perfusion (ASCP), an adjunctive technique to deep hypothermic circulatory arrest (DHCA), has been applied for cerebral protection during aortic arch repair surgery. Evidences from several studies have indicated that ASCP

**Address for correspondence:** Prof. Jin-Ping Liu,

Department of Cardiopulmonary Bypass, Cardiovascular Institute, Fuwai Hospital and National Center for Cardiovascular Diseases, Beijing 100037, China  
E-Mail: jinpingsfw@hotmail.com

This is an open access article distributed under the terms of the Creative Commons Attribution-NonCommercial-ShareAlike 3.0 License, which allows others to remix, tweak, and build upon the work non-commercially, as long as the author is credited and the new creations are licensed under the identical terms.

**For reprints contact:** reprints@medknow.com

© 2016 Chinese Medical Journal | Produced by Wolters Kluwer - Medknow

**Received:** 03-11-2015 **Edited by:** Li-Min Chen

**How to cite this article:** Zou LH, Liu JP, Zhang H, Wu SB, Ji BY. Cerebral Metabolic Profiling of Hypothermic Circulatory Arrest with and Without Antegrade Selective Cerebral Perfusion: Evidence from Nontargeted Tissue Metabolomics in a Rabbit Model. Chin Med J 2016;129:702-8.

Access this article online

Quick Response Code:



Website:  
www.cmj.org

DOI:  
10.4103/0366-6999.178012

performs cerebral protection during the aortic arch repair surgery.<sup>[1-5]</sup> However, brain metabolism profile after ASCP has not been systematically investigated by metabolomics technology.

Metabolites in tissues could accurately reflect the status of the biological system as the end results of metabolism. The metabolic profile of brain after ASCP may reveal new insight into cerebral protective mechanisms. Metabolomics is regarded as a useful tool for revealing the cerebral metabolic profiling as the advantage of comprehensive and quantitative analysis of global metabolites. In the present study, we compared the metabolic characteristics of the brain tissues between DHCA rabbits with and without ASCP by the virtue of gas chromatography-mass spectrometry (GC/MS). We hypothesized that cerebral metabolism reflected by carbohydrates, amino acids (AAs), and lipids could be better preserved by ASCP in a rabbit model.

## METHODS

### Chemical

All chemicals were reagent grades and obtained from commercial sources. Bis-trimethylsilyl-trifluoroacetamide (BSTFA), a derivatization reagent, was purchased from REGIS Technologies Inc., (USA), and 2-chloro-L-phenylalanine (number 103616-89-3) was purchased from Hengbo Corporation (Shanghai, China).

### Animals and grouping schedules

The experimental protocols were reviewed and approved by the Animal Ethics Committee of the Animal Experimental Center in Fuwai Hospital (Ethical Code: 2013-4-150-GZR). Twelve adult male New Zealand rabbits (15–20 weeks, 2.1–3.7 kg) were randomly divided into DHCA group ( $n = 6$ , D group) or DHCA + ASCP group ( $n = 6$ , DA group) and another 12 rabbits were used as blood donors during cardiopulmonary bypass (CPB).

The procedure was performed according to the previous studies.<sup>[6-8]</sup> Animals were anesthetized with sodium pentobarbital (20 mg/kg, intravenous injection), then incubated with a 3.5 F trachea cannula, and ventilated with a respirator (ELISA, Kronberg, German). The left femoral artery was catheterized for arterial pressure monitoring and blood sample collection for blood gas analysis. The CPB included a twin-roller pump (Stöckert, Munich, German), a Capiox Baby FX05 membrane oxygenator, a heat-cooler system (Maquet, Jostra HCU30), and a reservoir. The priming solution was composed of succinylated gelatin, plasmalyte-A, sodium bicarbonate, and 45 ml fresh whole blood from donor rabbits, and the total priming volume was about 70 ml. After activated clotting time reached above 480 s, CPB was initiated by cannulation on right atrium and right subclavian for venous drainage and artery inflow, respectively. Cardiac arrest was conducted by perfusion of histidine-tryptophan-ketoglutarate solution (40 ml/kg) after aortic cross-clamping when the rectal temperature was decreased to 30°C. DHCA was initiated as well as

the rectal temperature was decreased to 20°C. Rabbits in group D were performed DHCA alone, and rabbit in group DA were performed DHCA with ASCP by occluding the innominate artery with flow rate at 10 ml·kg<sup>-1</sup>·min<sup>-1</sup>.<sup>[6]</sup> The duration of ASCP and DHCA were maintained for 60 min. The ascending aorta was reopened when the rectal temperature was recovered to 30°C. Rabbits were weaned off CPB when the rectal temperature was 37°C and hemodynamics were stable. The rabbit cerebral cortex was harvested for metabolomics analysis at 60 min after weaning off CPB [Figure 1].

### Tissue sample pretreatment for metabolomics

Metabolomics analyses were performed by GC/MS, the methods of which have been described previously.<sup>[9-11]</sup> Rabbit brain tissue (100 mg) was collected in 2 ml sealed vials and stored at -80°C until it was removed into a 2 ml tube for analysis. Both 50 µl of L-2-chlorophenylalanine (0.1 mg/ml stock in dH<sub>2</sub>O), as an internal standard, and 0.5 ml of the extraction liquid ( $v_{\text{methanol}}: v_{\text{chloroform}} = 3:1$ ) were added into the tube. To homogenize the tissue, steel balls were placed into the sample tubes. The sample was homogenized for 7 min at 55 Hz, then centrifuged for 15 min at 12,000 r/min. The 0.4 ml supernatant was transferred into a fresh 2 ml GC/MS glass vial and lyophilized in a vacuum concentrator. The dried supernatant was mixed with 80 µl of methoxyamination reagent (20 mg/ml in pyridine) and incubated for 2 h at 37°C. Total 0.1 ml BSTFA reagent (1% TMCS, v/v) was added to the sample aliquots, then incubated for 1 h at 70°C. GC/MS analysis was performed when the temperatures were decreased to the room temperature.

### Metabolomic analysis by gas chromatography-mass spectrometry

GC/time-of-flight (TOF) MS analysis was performed applying an Agilent 7890A (Agilent Technologies, USA) gas chromatograph system coupled with a Pegasus HT time-of-flight mass spectrometer (LECO Chroma TOF Pegasus HT, LECO, USA). The system utilized a Agilent DB-5MS capillary column coated with 5% diphenyl cross-linked with 95% dimethylpolysiloxane (30 m × 250 µm inner diameter, 0.25 µm film thickness; J and W Scientific, Folsom, CA, USA). 1 µl aliquot of the analyte was injected in splitless mode. Helium was used as the carrier gas, and the front inlet purge flow was 3 ml/min, and the gas flow rate through the column was 20 ml/min. Before being raised to 330°C at a rate of 10°C/min, the initial temperature was kept at 50°C for 1 min, then the temperature was maintained for 5 min at 330°C. The injection, transfer line, and ion source temperatures were 280, 280, and 220°C, respectively. The energy was -70 eV in electron impact mode. The MS data were acquired in a full-scan mode with the m/z range of 30–600 at a rate of 20 spectra/s after a solvent delay of 366 s.

### Metabolite identification

The LECO/Fiehn Metabolomics Library was used to identify the compounds,<sup>[12]</sup> which would give a similarity value for

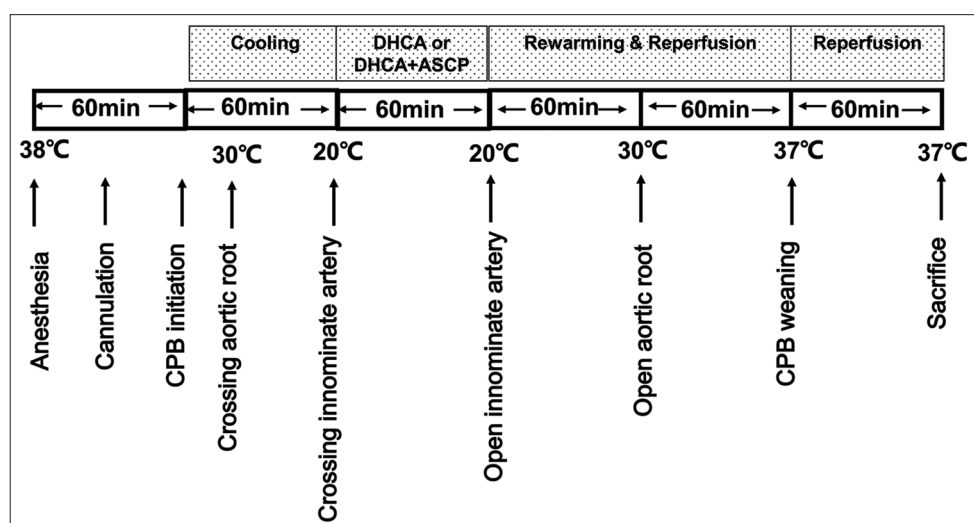


**Figure 1:** The protocol of ASCP model. DHCA: Deep hypothermic circulatory arrest; ASCP: Antegrade selective cerebral perfusion; CPB: Cardiopulmonary bypass.

the compound identification accuracy. If the similarity is more than 700, the metabolite identification is reliable. If the similarity is less than 200, the library would only use “analyte” for the compound name. If the similarity is between 200 and 700, the compound name is a putative annotation.

### Data processing and statistical analysis

The data were analyzed according to the previous studies.<sup>[9,13]</sup> Internal standard normalization method was employed in this data analysis. The three-dimensional data involving the peak number, sample name, and normalized peak area were fed to SIMCA-P 13.0 software package (Umetrics, Umea, Sweden) for principal component analysis (PCA), and partial least squares-DA (PLS-DA). Several parameters, including  $R^2X$ ,  $R^2Y$ ,  $Q^2Y$ -intercepts, were used to evaluate the validity and over-fitting of the model. Based on the orthogonal projections to latent structures-DA, a loading plot was constructed, which showed the contribution of variables to difference between two groups. It also showed the important variables which were situated far from the origin, but the loading plot is complex because of many variables. To refine this analysis, the first principal component ( $t_1$ ) of variable importance projection (VIP) was obtained. The VIP values exceeding 1.0 were selected as potentially changed metabolites.

The variables were then assessed by Student’s  $t$ -test using SPSS 16.0 (SPSS Inc., Chicago, IL, USA),  $P < 0.05$  was considered statistically significant, whereas variables with  $P > 0.05$  were discarded between two comparison groups.

### Pathway analysis

To evaluate the metabolic change associated with ASCP, metabolic pathway analysis was performed using the significantly changed metabolites determined by Student’s  $t$ -test. In our study, Kyoto Encyclopedia of Genes and Genomes (KEGG) (<http://www.genome.jp/kegg/>) was utilized to search for the pathways of metabolite which is a commercial database and also used for pathway analysis previously.<sup>[9]</sup>

## RESULTS

### Multivariate analysis

In the present study, metabolomics characteristic was analyzed by a nontargeted metabolomics strategy (GC-MS). The MS data indicating the metabolic characteristic were analyzed by SIMCA-P. PCA showed the distribution of origin data. In order to obtain a higher level of group separation and get a better understanding of variables responsible for classification, a supervised PLS-DA was applied. The results showed that group DA was separated from group D by first principal component ( $t_1$ ) [Figure 2]. The parameters of PLS-DA for the classification from the software were  $R^2X = 0.441$ ,  $R^2Y = 0.996$ , and  $Q^2Y = 0.88$ . A leave-one-out validation was further used to estimate the robustness and the predictive ability of the model, which was proceeded in order to further validate the model. The  $R^2$  and  $Q^2$  intercepts were 0.922 and 0.229 after 200 permutations, respectively [Figure 3]. The values of  $Q^2$  intercept indicated the robustness of the models, thus which showed a low risk of overfitting and reliable. The results above strongly verified the model validity.

### Differential metabolites between deep hypothermic circulatory arrest and deep hypothermic circulatory arrest + antegrade selective cerebral perfusion groups

The metabolic profiles in the DA group substantially differed from the D group. Missing values of raw data were filled up by half of the minimum value. Metabolites with both VIP more than one and  $P < 0.05$  would be selected for further identification. We found that 62 endogenous biochemical markers were identified to be significantly different between D group and DA group [Supplementary Table 1]. Major changes were observed in AAs, followed by carbohydrates and then lipids. Nucleotides, cofactors and vitamins, energy substrate, and peptides were also changed significantly, and the names of which were presented in Supplementary Table 1.

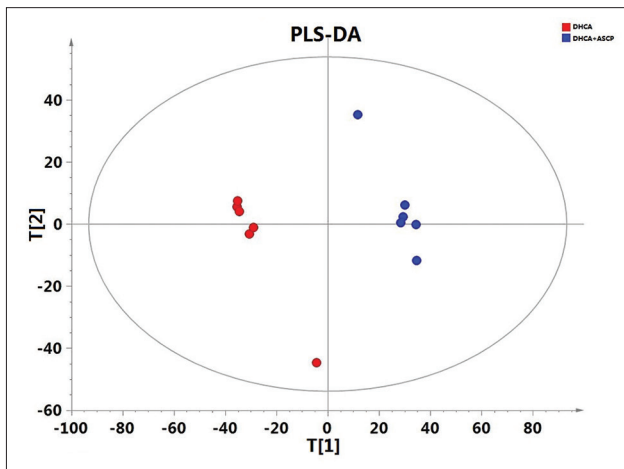


**Figure 2:** Score plots of PLS-DA. Score plot of PLS-DA model was obtained from DHCA and DHCA + ASCP group.  $R^2X = 0.441$ ,  $R^2Y = 0.996$  and  $Q^2Y = 0.88$ . DHCA: Deep hypothermic circulatory arrest; PLS-DA: Partial least squares-discriminant analysis; ASCP: Antegrade selective cerebral perfusion.

### Metabolic pathway

All 62 different metabolites between the two groups were searched in an online database (KEGG, <http://www.genome.jp/kegg/>), and 43 metabolites were found in the KEGG metabolic pathways [Supplementary Table 1]. A map of ASCP-related metabolic pathways was plotted according to the most relevant distinguishing metabolites [Figure 4].

Compared to D group, metabolic pathways in DA group were characterized by activation of the glycolytic pathway with the increase in glucose-6-phosphate and glucose-1-phosphate, whereas anaerobic metabolism reflecting by decreased lactic acid production was inhibited in the early stage after ASCP. The level of glucose and pyruvate were not changed between the two groups, whereas the glucose catabolites (such as sorbitol, D-myo-inositol, and fructose) were increased significantly in DA group. Metabolites on tricarboxylic acid cycle (TAC) were not significantly different after reperfusion between the two groups, whereas several intermediates including oxalic acid and 2-hydroxybutanoic acid were higher in DA group comparing to D group [ $P$  values were displayed in Supplementary Table 1].

The levels of several AAs (serine, methionine, cysteine, glycine, glutamine, glutamic acid, and aspartate) were decreased in the DA group, some of which involved in oxidative stress, such as glutamine, glutamic acid, glycine, and aspartate [ $P$  values were displayed in Supplementary Table 1]. Tryptophan known as a kind of aromatic amino acids showed no difference between the two groups, but its metabolites including L-kynurenine (KYN,  $P = 0.0019$ ), 5-methoxyindole-3-acetic acid ( $P = 0.0499$ ), and 5-hydroxyindole-3-acetic acid ( $P = 0.0495$ ) were decreased significantly in DA group, which had been demonstrated to be related to cerebral injury.<sup>[14]</sup> Furthermore, citrulline in urea cycle was found to be increased ( $P = 0.0158$ ).

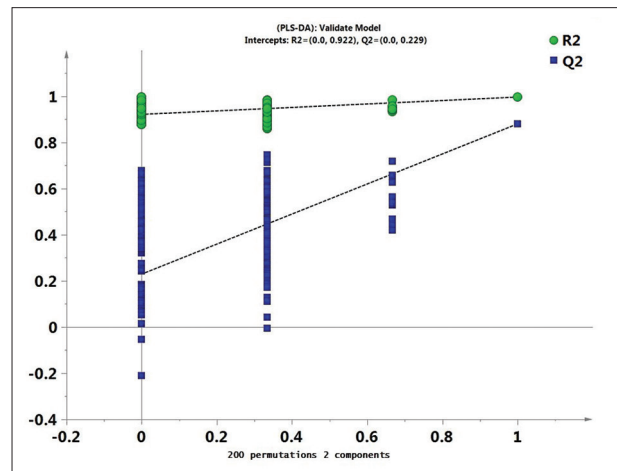


**Figure 3:** Permutation test of a leave-one-out validation model. Validation was obtained from 200 permutations test for the same comparisons, and the resulting  $R^2$  (green triangle) and  $Q^2$  (blue square) values were plotted. The green line represents the regression line for  $R^2$  and the blue line for  $Q^2$ . The  $R^2$  (goodness of the fit) and  $Q^2$  (goodness of the prediction) intercept values were 0.922 and 0.229, respectively.

There were also significant different changes in the metabolites involved in lipid metabolism between group DA and group D. Metabolomics analysis identified increased levels of 3,7,12-trihydroxycoprostone, cis-gondoic acid, gluconic lactone, methyl jasmonate, and heptadecanoic acid. The level of O-phosphorylethanolamine, palmitoleic acid, and palmitic acid were decreased in DA group [ $P$  values were displayed in Supplementary Table 1].

### DISCUSSION

In this study, we focused metabolism profile alteration in the early stage after DHCA with and without ASCP in a rabbit model and yielded fundamental insights into metabolic pathways related to ASCP. In the previous study, several methods have been applied for cerebral metabolism research during ASCP including positron emission tomography, diffusion-weighted imaging, proton magnetic resonance spectroscopy, and microdialysis.<sup>[5,15]</sup> However, few study explored cerebral metabolism after ASCP with metabolomics. Currently, metabolomics is applied for describing the metabolic profile in neurology researches such as stroke and Alzheimer's disease,<sup>[9,16]</sup> as its comprehensive and quantitative advantage. In addition, GC-MS is of excellent sensitivity and resolution for chemical analysis in metabolomics,<sup>[17-19]</sup> and applied in our study to explore the effects of ASCP on the metabolism profile in the brain. In the present study, 62 definable metabolites were varied significantly after ASCP, which were mainly related to amino acid metabolism, carbohydrate metabolism, and lipid metabolism.

Brain energy supply has been thought to depend on glucose oxidative metabolism from glycolytic processes. In Cavus *et al.* study, they found that the level of cerebral glucose and pyruvate were higher during ASCP compared to that during circulatory arrest, but there were no differences of glucose

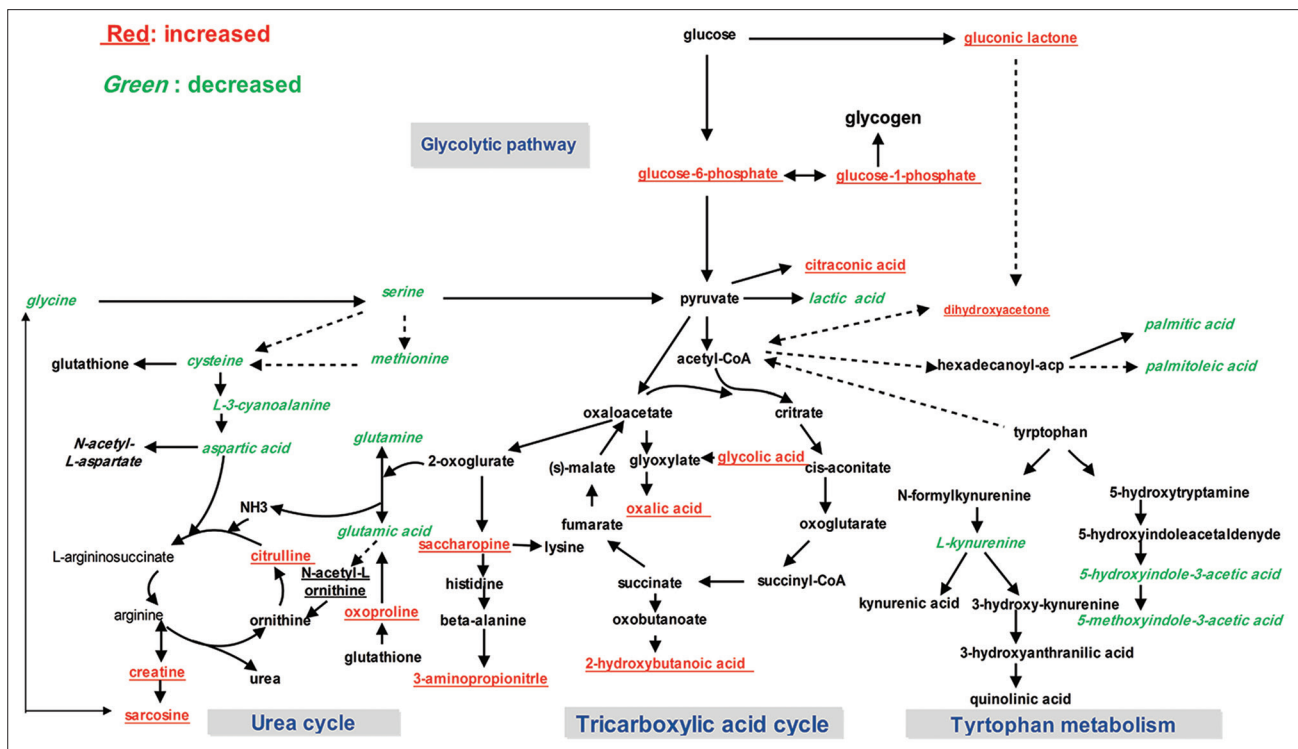


**Figure 4:** Changed metabolites and altered metabolic pathways for the most relevant distinguishing metabolites in the brain during antegrade selective cerebral perfusion. Red metabolites with an underline are upregulated, and green metabolites with italic are downregulated in DA group comparing to D group. Dotted arrows represent multiple steps. TAC: Tricarboxylic acid cycle; DA: Discriminant analysis.

and pyruvate between the reperfusion phase after DHCA and ASCP. Accordingly, we demonstrated that glucose and pyruvate showed no difference between the early stage after ASCP and DHCA, indicating that the energy supply in D group is recovered rapidly after the reperfusion is restored, thus there is no difference in the glucose and pyruvate between group AD and group D. In addition, we found that glucose-6-phosphate and glucose-1-phosphate in glycolytic pathway were increased significantly in DA group, as well as the TAC products such as oxalate and 2-hydroxybutanoic acid.

In our study the lactic acid from glycolytic pathway was observed to be decreased in group DA, and previous studies have demonstrated that lactic acid produced from anaerobic glycolysis in astrocytes provides the primary metabolic fuel for neurons<sup>[20]</sup> and is an essential element of neuron-glia metabolic interactions<sup>[21,22]</sup> as an alternative energy substrate for brain metabolism in the absence of oxygen.<sup>[20]</sup> In the piglet model with DHCA, the level of lactate was observed to be persistently increased during the early stage after DHCA, whereas ASCP could attenuate this trend.<sup>[23]</sup> Consistently, jugular bulb pH was found to be significantly higher after ASCP comparing with DHCA<sup>[24]</sup> that is accordance with Hagl's *et al.* study, in which a lower pH could be observed even 4 h after DHCA, and ASCP could attenuate the acidosis.<sup>[25]</sup> Hence, the decrease of lactic acid in group DA indicated that ASCP may improve the acid-base balance and alleviated acidosis induced by DHCA.

Oxidative stress has been demonstrated to be increased during CPB.<sup>[26]</sup> The brain is especially susceptible to oxidative stress due to abundant lipid content in myelin sheaths, and antioxidant level has been demonstrated to be related to postoperative delirium in patients undergoing CPB surgery.<sup>[27]</sup> Cerebral damage induced by oxidative stress during DHCA attracts lots of attention, and excitatory amino acids were observed to increase significantly after DHCA.<sup>[28]</sup> Glutamate excitotoxicity was observed to be related to neuronal apoptosis and necrosis after hypothermic circulatory arrest.<sup>[29]</sup> In our study, several excitatory amino acids relating to oxidative stress were decreased in the DA group, including glutamine, glutamic acid, and aspartate, in which glutamine is the main precursor for excitatory neuromediator glutamate and inhibitory neurotransmitter  $\gamma$ -aminobutyric acid.<sup>[30]</sup> The decrease of excitatory amino acid (EAA) after ASCP may provide further evidence for the protective effect of ASCP.

In addition, several studies have showed that tryptophan loading could induce oxidative stress in brain cortex of rats, and tryptophan metabolism may contribute to brain damage following stroke.<sup>[31,32]</sup> In the present study, we determined that several tryptophan metabolites were decreased during the early stage after ASCP that may alleviate brain oxidative damage. Besides, KYN has been known to play an important role in the process of neuronal damage and neurodegenerative disorders, and it could promote oxidative stress following a stroke.<sup>[31]</sup> In addition,

we found that citrulline in urea cycle was also increased at the early stage after ASCP, but the exact mechanism of this effect need further study.

In our study, the change of cerebral glycerol was not determined in the early stage after ASCP, but the alteration of several long-chain fatty acid and metabolites were observed. Palmitic acid was observed to be decreased after ASCP, which has been demonstrated to induce cell death associated with trauma in the central nervous system.<sup>[33]</sup>

There are also several limitations in the present study. First of all, although metabolomics was applied to observe brain tissues metabolism in the rabbit ASCP model, metabolites alteration in plasma and cerebrospinal fluid were not determined simultaneously by metabolomics. In the further study, metabolic profile between the two groups should be observed for a longer time. In addition, targeted metabolomics may be required for further verify of the metabolites with a significant difference in the present study, what is more underlying mechanism for the cerebral metabolism after ASCP required further studied.

In conclusion, the present study clarify the cerebral metabolic profiling in DHCA rabbits with and without ASCP using metabolomics analysis, and the results may shed new lights that cerebral metabolism is better preserved by DHCA with ASCP comparing to DHCA alone, but further studies are necessary to reveal the underlying mechanism.

*Supplementary information is linked to the online version of the paper on the Chinese Medical Journal website.*

## Acknowledgments

Metabolomics analysis was supported by Shanghai Biotree Biotechnology, and the authors acknowledge Jun-Liang Deng for the measurement of metabolites using GC-MS and assistance in statistical analysis. We do appreciate Mohsen Ahmadian (Hampson English School) and You-Zhou Chen (Beijing Jishuitan Hospital) for their help in language editing.

## Financial support and sponsorship

This work was supported by the grants from National Natural Science Foundation of China (No. 81370351 and No. 81270225).

## Conflicts of interest

There are no conflicts of interest.

## REFERENCES

1. Di Eusano M, Schepens M, Morshuis W, Dossche K, Pacini D, Di Marco L, *et al.* Operations on the thoracic aorta and antegrade selective cerebral perfusion: Our experience with 462 patients. *Ital Heart J* 2004;5:217-22.
2. Di Eusano M, Schepens MA, Morshuis WJ, Di Bartolomeo R, Pierangeli A, Dossche KM. Antegrade selective cerebral perfusion during operations on the thoracic aorta: Factors influencing survival and neurologic outcome in 413 patients. *J Thorac Cardiovasc Surg* 2002;124:1080-6. doi: 10.1067/mtc.2002.124994.
3. Di Eusano M, Schepens MA, Morshuis WJ, Dossche KM, Di Bartolomeo R, Pacini D, *et al.* Brain protection using antegrade

- selective cerebral perfusion: A multicenter study. *Ann Thorac Surg* 2003;76:1181-8. doi: 10.1016/S0003-4975(03)00824-5.
4. Kazui T, Yamashita K, Washiyama N, Terada H, Bashar AH, Suzuki T, *et al.* Usefulness of antegrade selective cerebral perfusion during aortic arch operations. *Ann Thorac Surg* 2002;74:S1806-9. doi: 10.1016/S0003-4975(02)04150-4.
5. Liang MY, Tang ZX, Chen GX, Rong J, Yao JP, Chen Z, *et al.* Is selective antegrade cerebral perfusion superior to retrograde cerebral perfusion for brain protection during deep hypothermic circulatory arrest? Metabolic evidence from microdialysis. *Crit Care Med* 2014;42:e319-28. doi: 10.1097/ccm.0000000000000220.
6. Zou L, Liu J, Zhang H, Wu S, Long C, Ji B, *et al.* A rabbit model of antegrade selective cerebral perfusion with cardioplegic arrest. *Perfusion* 2015. pii: 0267659115599835. doi: 10.1177/0267659115599835.
7. Pan X, Sun L, Ma W, Tang Y, Long C, Tian L, *et al.* Overactivation of poly (adenosine phosphate-ribose) polymerase 1 and molecular events in neuronal injury after deep hypothermic circulatory arrest: Study in a rabbit model. *J Thorac Cardiovasc Surg* 2007;134:1227-33. doi: 10.1016/j.jtcvs.2007.05.062.
8. Wang Q, Yang J, Long C, Zhao J, Li Y, Xue Q, *et al.* Hyperoxia management during deep hypothermia for cerebral protection in circulatory arrest rabbit model. *ASAIO J* 2012;58:330-6. doi: 10.1097/MAT.0b013e318251dfab.
9. Hu ZP, Browne ER, Liu T, Angel TE, Ho PC, Chan EC. Metabonomic profiling of TASTPM transgenic Alzheimer's disease mouse model. *J Proteome Res* 2012;11:5903-13. doi: 10.1021/pr300666p.
10. Nesnow S, Padgett WT, Moore T. Propiconazole induces alterations in the hepatic metabolome of mice: Relevance to propiconazole-induced hepatocarcinogenesis. *Toxicol Sci* 2011;120:297-309. doi: 10.1093/toxsci/kfr012.
11. Wu R, Wu Z, Wang X, Yang P, Yu D, Zhao C, *et al.* Metabonomic analysis reveals that carnitines are key regulatory metabolites in phase transition of the locusts. *Proc Natl Acad Sci U S A* 2012;109:3259-63. doi: 10.1073/pnas.1119155109.
12. Kind T, Wohlgemuth G, Lee do Y, Lu Y, Palazoglu M, Shahbaz S, *et al.* FiehnLib: Mass spectral and retention index libraries for metabolomics based on quadrupole and time-of-flight gas chromatography/mass spectrometry. *Anal Chem* 2009;81:10038-48. doi: 10.1021/ac9019522.
13. Agudo-Barriuso M, Lahoz A, Nadal-Nicolás FM, Sobrado-Calvo P, Piquer-Gil M, Diaz-Llopis M, *et al.* Metabonomic changes in the rat retina after optic nerve crush. *Invest Ophthalmol Vis Sci* 2013;54:4249-59. doi: 10.1167/iovs.12-11451.
14. Mackay GM, Forrest CM, Stoy N, Christofides J, Egerton M, Stone TW, *et al.* Tryptophan metabolism and oxidative stress in patients with chronic brain injury. *Eur J Neurol* 2006;13:30-42. doi: 10.1111/j.1468-1331.2006.01220.x.
15. Pacini D, Di Marco L, Leone A, Tonon C, Pettinato C, Fonti C, *et al.* Cerebral functions and metabolism after antegrade selective cerebral perfusion in aortic arch surgery. *Eur J Cardiothorac Surg* 2010;37:1322-31. doi: 10.1016/j.ejcts.2009.12.029.
16. Irie M, Fujimura Y, Yamato M, Miura D, Wariishi H. Integrated MALDI-MS imaging and LC-MS techniques for visualizing spatiotemporal metabolomic dynamics in a rat stroke model. *Metabolomics* 2014;10:473-483. doi: 10.1007/s11306-013-0588-8.
17. Li J, Ren L, Sun G, Huang H. Gas chromatography-mass spectrometry (GC-MS) and its application in metabonomics. *Sheng Wu Gong Cheng Xue Bao* 2013;29:434-46. doi: 13345/j.cjb.2013.04.009.
18. Patti GJ. Separation strategies for untargeted metabolomics. *J Sep Sci* 2011;34:3460-9. doi: 10.1002/jssc.201100532.
19. Wilson ID, Nicholson JK, Castro-Perez J, Granger JH, Johnson KA, Smith BW, *et al.* High resolution "ultra performance" liquid chromatography coupled to oa-TOF mass spectrometry as a tool for differential metabolic pathway profiling in functional genomic studies. *J Proteome Res* 2005;4:591-8. doi: 10.1021/pr049769r.
20. Chih CP, Roberts EL Jr. Energy substrates for neurons during neural activity: A critical review of the astrocyte-neuron lactate shuttle hypothesis. *J Cereb Blood Flow Metab* 2003;23:1263-81. doi: 10.1097/01.wcb.0000081369.51727.6f.
21. Pellerin L. Lactate as a pivotal element in neuron-glia metabolic cooperation. *Neurochem Int* 2003;43:331-8. doi:10.1016/S0197-0186(03)00020-2.

22. Schurr A. Lactate, glucose and energy metabolism in the ischemic brain (Review). *Int J Mol Med* 2002;10:131-6. doi:10.3892/ijmm.10.2.131.
23. Cavus E, Hoffmann G, Bein B, Scheewe J, Meybohm P, Renner J, *et al.* Cerebral metabolism during deep hypothermic circulatory arrest vs moderate hypothermic selective cerebral perfusion in a piglet model: A microdialysis study. *Paediatr Anaesth* 2009;19:770-8. doi: 10.1111/j.1460-9592.2009.03074.x.
24. Harrington DK, Walker AS, Kaukuntla H, Bracewell RM, Clutton-Brock TH, Faroqui M, *et al.* Selective antegrade cerebral perfusion attenuates brain metabolic deficit in aortic arch surgery: A prospective randomized trial. *Circulation* 2004;110 11 Suppl 1:II231-6. doi: 10.1161/01.CIR.0000138945.78346.9c.
25. Hagl C, Khaladj N, Peterss S, Hoeffler K, Winterhalter M, Karck M, *et al.* Hypothermic circulatory arrest with and without cold selective antegrade cerebral perfusion: Impact on neurological recovery and tissue metabolism in an acute porcine model. *Eur J Cardiothorac Surg* 2004;26:73-80. doi: 10.1016/j.ejcts.2004.04.002.
26. Ulus AT, Aksoyek A, Ozkan M, Katircioglu SF, Vessby B, Basu S. Oxidative stress and changes in alpha- and gamma-tocopherol levels during coronary artery bypass grafting. *Ann N Y Acad Sci* 2004;1031:352-6. doi: 10.1196/annals.1331.043.
27. Karlidag R, Unal S, Sezer OH, Bay Karabulut A, Battaloglu B, But A, *et al.* The role of oxidative stress in postoperative delirium. *Gen Hosp Psychiatry* 2006;28:418-23. doi: 10.1016/j.genhosppsych.2006.06.002.
28. Zhu M, Zhao Y, Zheng Y, Su D, Wang X. Relative higher hematocrit attenuates the cerebral excitatory amino acid elevation induced by deep hypothermic circulatory arrest in rats. *Ther Hypothermia Temp Manag* 2013;3:140-2. doi: 10.1089/ther.2013.0004.
29. Tseng EE, Brock MV, Lange MS, Troncoso JC, Blue ME, Lowenstein CJ, *et al.* Glutamate excitotoxicity mediates neuronal apoptosis after hypothermic circulatory arrest. *Ann Thorac Surg* 2010;89:440-5. doi: 10.1016/j.athoracsur.2009.10.059.
30. Hertz L, Zielke HR. Astrocytic control of glutamatergic activity: Astrocytes as stars of the show. *Trends Neurosci* 2004;27:735-43. doi: 10.1016/j.tins.2004.10.008.
31. Darlington LG, Mackay GM, Forrest CM, Stoy N, George C, Stone TW. Altered kynurenine metabolism correlates with infarct volume in stroke. *Eur J Neurosci* 2007;26:2211-21. doi: 10.1111/j.1460-9568.2007.05838.x.
32. Feksa LR, Latini A, Rech VC, Feksa PB, Koch GD, Amaral MF, *et al.* Tryptophan administration induces oxidative stress in brain cortex of rats. *Metab Brain Dis* 2008;23:221-33. doi: 10.1007/s11011-008-9087-4.
33. Ulloa JE, Casiano CA, De Leon M. Palmitic and stearic fatty acids induce caspase-dependent and -independent cell death in nerve growth factor differentiated PC12 cells. *J Neurochem* 2003;84:655-68. doi: 10.1046/j.1471-4159.2003.01571.x.

**Supplementary Table 1: Identification results of significant metabolites in brain tissue between DHCA group and DHCA + ASCP group**

Metabolite	tR (min)	Mass	SD	VIP	P <sup>t</sup>	Log <sub>2</sub> fold change*	Pathway
Glutamine	15.67	257	3.23	2.59	0.0018	-20.59	map00230 Purine metabolism
Aspartic acid	12.37	116	2.64	1.22	0.0153	-1.61	map00250 Alanine, aspartate and glutamate metabolism
Serine	10.14	143	2.87	1.50	0.0123	-3.00	map00260 Glycine, serine and threonine metabolism
L-cysteine	13.98	220	3.76	2.99	0.0013	-3.17	map00260 Glycine, serine and threonine metabolism
Sarcosine	8.39	267	3.09	2.88	0.0001	19.55	map00260 Glycine, serine and threonine metabolism
Creatine	13.91	102	3.10	2.05	0.0371	20.34	map00260 Glycine, serine and threonine metabolism
Methionine	13.54	176	3.63	2.92	0.0008	-4.08	map00270 Cysteine and methionine metabolism
Citraconic acid	11.58	144	3.10	2.46	0.0013	3.10	map00290 Valine, leucine and isoleucine biosynthesis
Saccharopine	23.18	199	3.26	2.62	0.0008	20.77	map00300 Lysine biosynthesis
Citrulline	16.98	157	2.82	1.55	0.0158	1.31	map00330 Arginine and proline metabolism
5-hydroxyindole-3-acetic acid	20.72	290	2.72	1.56	0.0495	-18.99	map00380 Tryptophan metabolism
L-kynurenine	20.30	174	3.01	1.97	0.0019	-3.70	map00380 Tryptophan metabolism
5-methoxyindole-3-acetic acid	20.34	156	2.72	1.44	0.0499	-18.72	map00380 Tryptophan metabolism
N-methyl-L-glutamic acid	12.86	98	3.21	2.58	0.0013	-20.48	map00680 Methane metabolism
8-aminocaprylic acid	18.14	223	3.13	2.92	0.0025	19.72	Null number
N(alpha),N(alpha)-dimethyl-L-histidine	16.95	214	3.09	2.42	0.0025	19.32	Null number
Glutamic acid	14.57	156	3.52	2.38	0.0042	-2.57	Null number
Glycine	10.78	370	2.82	1.44	0.0135	-4.64	Null number
Glucuronic acid	17.74	182	3.37	2.72	0.0001	4.19	map00040 Pentose and glucuronate interconversions
Fructose	17.36	273	3.18	2.97	0.0146	20.18	map00051 Fructose and mannose metabolism
Sorbitol	18.03	157	3.31	2.21	0.0055	4.65	map00051 Fructose and mannose metabolism
Myo-inositol	19.62	150	3.75	2.55	0.0022	2.63	map00052 Galactose metabolism
Glycolic acid	7.28	100	3.78	3.53	0.0025	24.00	map00361 Chlorocyclohexane and chlorobenzene degradation
Ethanolamine	10.23	319	3.15	2.14	0.0205	20.63	map00440 Phosphonate and phosphinate metabolism
Cellobiose	24.60	214	2.64	1.83	0.0170	17.26	map00500 Starch and sucrose metabolism
Alpha-D-glucosamine 1-phosphate	16.75	232	2.65	1.76	0.0108	17.17	map00520 Amino sugar and nucleotide sugar metabolism
Dihydroxyacetone	10.00	231	2.64	1.76	0.0363	17.26	map00561 Glycerolipid metabolism
Oxalic acid	8.10	114	3.04	1.79	0.0097	4.03	map00625 Chloroalkane and chloroalkene degradation
2-hydroxybutanoic acid	8.21	131	2.51	1.19	0.0082	1.96	map00640 Propanoate metabolism

Contd...

Supplementary Table 1: Contd...

Metabolite	tR (min)	Mass	SD	VIP	P <sup>†</sup>	Log <sub>2</sub> fold change*	Pathway
Lactic acid	7.14	102	3.15	2.49	0.0014	-2.82	Null number
Lactitol	24.98	191	3.00	1.94	0.0222	2.56	Null number
Glucose-6-phosphate	21.59	123	3.21	2.11	0.0228	4.53	Null number
DL-dihydrosphingosine	22.82	204	2.93	1.49	0.0126	2.43	Null number
Glucose-1-phosphate	16.37	217	1.29	1.29	0.0303	1.67	Null number
Gluconic lactone	17.76	204	2.56	1.14	0.0059	1.22	map00030 Pentose phosphate pathway
Palmitoleic acid	19.02	211	2.88	1.41	0.0376	-3.05	map00061 Fatty acid biosynthesis
Palmitic acid	19.20	225	3.24	2.50	0.0119	-20.51	map00061 Fatty acid biosynthesis
O-phosphorylethanolamine	16.55	216	2.71	1.49	0.0211	-1.48	map00564 Glycerophospholipid metabolism
Methyl jasmonate	15.53	180	2.87	1.84	0.0100	2.66	map00592 Alpha-linolenic acid metabolism
3,7,12-trihydroxycoprostanol	27.84	102	4.01	3.74	0.0019	25.43	Null number
cis-gondoic acid	22.42	221	3.00	1.96	0.0499	1.74	Null number
Heptadecanoic acid	19.97	156	3.00	1.50	0.0307	4.45	Null number
Adenine	17.48	264	3.39	2.25	0.0075	1.72	map00230 Purine metabolism
Inosine	23.49	221	2.28	1.07	0.0074	1.70	map00230 Purine metabolism
Cytidine-monophosphate	18.93	243	3.21	3.00	0.0000	20.15	map00240 Pyrimidine metabolism
Methylmalonic acid	9.44	216	2.93	1.50	0.0161	4.23	map00240 Pyrimidine metabolism
Isoxanthopterin	19.95	166	3.02	2.39	0.0158	-3.10	Null number
5,6-dihydrouracil	13.17	243	2.89	1.46	0.0203	-2.05	Null number
Oxoproline	13.60	160	3.50	3.26	0.0105	22.21	map00480 Glutathione metabolism
Acetophenone	9.52	162	2.72	1.04	0.0200	-2.16	map00642 Ethylbenzene degradation
Acenaphthenequinone	20.07	238	3.32	3.10	0.0041	-21.21	Null number
Ascorbate	18.11	244	3.24	1.78	0.0213	1.39	Null number
Phosphate	10.38	98	3.80	3.55	0.0240	24.23	map00190 Oxidative phosphorylation
3-aminopropionitrile	13.33	199	3.33	2.12	0.0478	2.71	map00410 Beta-alanine metabolism
3-cyanoalanine	11.66	141	3.02	1.37	0.0364	-2.76	map00460 Cyanoamino acid metabolism
4-aminobenzoic acid	17.23	221	3.09	2.09	0.0034	2.17	map00627 Aminobenzoate degradation
Maleamate	12.54	216	2.94	1.87	0.0331	-2.32	map00760 Nicotinate and nicotinamide metabolism
Neohesperidin	23.06	117	3.05	2.45	0.0006	-19.40	map00941 Flavonoid biosynthesis
Piceatannol	23.15	98	2.93	1.90	0.0039	-3.40	map00945 Stilbenoid, diarylheptanoid and gingerol biosynthesis
Aminomalonic acid	12.90	218	3.28	2.19	0.0027	-1.90	Null number
Picolinic acid	11.13	180	2.84	1.88	0.0120	-18.45	Null number
2-amino-3-methyl-1-butanol	8.75	145	2.95	1.99	0.0091	-2.31	Null number

\*Fold changes when DHCA + ASCP group was compared to DHCA group; †P value was calculated using Student's *t*-test. VIP: Variable importance projection; tR: Retention time; DHCA: Deep hypothermic circulatory arrest; ASCP: Antegrade selective cerebral perfusion; SD: Standard deviation.